International Journal of Architectural, Civil and Construction Sciences
ISSN: 2415-1734
Vol:7, No:6, 2013

Study of Damage in Beams with Different Boundary Conditions

Nilson Barbieri and Renato Barbieri

***Abstract*—**In this paper the damage in clamped-free, clamped-clamped and free-free beam are analyzed considering samples without and with structural modifications. The damage location is investigated by the use of the bispectrum and wavelet analysis. The mathematical models are obtained using 2D elasticity theory and the Finite Element Method (FEM). The numerical and experimental data are approximated using the Particle Swarm Optimizer (PSO) method and this way is possible to adjust the localization and the severity of the damage. The experimental data are obtained through accelerometers placed along the sample. The system is excited using impact hammer.

***Keywords*—**Damage, beam, PSO, bispectrum, wavelet transform.

I. Introduction

An area of great interest in the field of engineering is the study and identification of structural damage [1]-[7].

Most identification techniques are based on modal parameters measured using only a few modes of vibration and/or modal frequencies of the structure that can easily be obtained by dynamic testing. The results are obtained with dynamic measurements at different times, corresponding to two moments of the life of the structure (usually with the model in good condition and damaged).

The methods based on dynamic tests do not require an analytical model of the structure, only some modal frequencies and mode shapes, before and after damage. The main methods based on vibration signals are: *Mode shape curvature method* [1], [3], [8]; *Change in flexibility method* [1], [3], [8]; *Change in flexibility curvature method* [1], [3], [8]; *Strain energy method* [1], [3]; *statistical methods* [1], [6], [9]-[14], and *wavelet analysis* [15]-[17]. Defects in components of machinery and structures can be detected by monitoring vibration. The bispectrum, a third-order statistic and kurtosis, a fourth-order moment, helps to identify faults in mechanical components. The bispectrum technique relates one set of mixing waves through the spectral coupling. The kurtosis gives an indication of the proportion of samples that deviate from the mean by a small value compared to those, which deviate by a large value [6], [11]-[14].

Nilson Barbieri is with the Pontifícia Universidade Católica do Paraná-PUCPR and Universidade Tecnológica Federal do Paraná-UTFPR, Curitiba, Paraná, BRASIL (Corresponding author. Phone: 55 41 32712211; fax: 55 41 32711349; e-mail: nilson.barbieri@pucpr.br).

Renato Barbieri is with Pontifícia Universidade Católica do Paraná – PUCPR, Curitiba, Paraná, BRASIL (e-mail: renato.barbieri@pucpr.br).

Another analysis procedure is the use of mathematical models tested. The correlation techniques are mixture of visual and numerical means to identify the differences between measurements and predictions. Whereas numerical correlation techniques return a numerical value, visual means of correlation are subjective and of qualitative nature [18]. Some of the basic correlation tools include simple tabulation or plotting the measured and predicted eingenvalues. A more strict correlation is the use of so-called "Modal Assurance Criteria" (MAC) [18]-[20].

The aim of this work is analyze structural changes through the inclusion of damage (crack) with known formats and positions in the samples. In this paper the damage in clamped-free, clamped-clamped and free-free beam are analyzed considering samples without and with structural modifications. The damage location is investigated varying the damage position in the mathematical model and comparing the numerical and experimental data. The mathematical models are obtained using the Finite Element Method (FEM). The experimental data are obtained using the impact hammer and laser velocity transducer. The statistics procedures are used to qualitative analysis.

To approximate the experimental and numeric FRF data, the Particle Swarm Optimizer (PSO) method is used. The first approximations of the position of the damage are obtained using two different parameters based in the energy of the signal and using bispectrum and wavelet analysis. Using this procedure and making a sweep of the modified finite element position along the sample, it is possible to identify with great precision the location and severity of the damage through the comparison of the experimental and numeric modal parameters.

II. Statistical and Modal Analysis

A. Bispectrum Theory

A quadratic non-linearity will relate three wave components in such a way that

$$X_m = \sum_{m=k+l} A_{k,l} X_k X_l + \varepsilon \tag{1}$$

where X_k and X_l denote the complex Fourier spectral components at ω_k and ω_l, with phase θ_k and θ_l, respectively. $A_{k,l}$ denotes the coupling coefficient and is dependent on the properties of the non-linearity system. The term ε denotes any errors associated with this model. In this system X_k and X_l will interact to create a third component X_m, where $\omega_m = \omega_k \pm \omega_l$ and $\theta_m = \theta_k \pm \theta_l$.

The bispectrum is defined as:

$$b(k,l) = X_k X_l X_m^* \tag{2}$$

where X_m^* denotes the complex conjugate of X_m. It can be clearly seen how this takes into account the mixing between two frequencies. If ω_k, ω_l and ω_{k+l} are independent, each will have an independent random phase (relative to each other).

The probability distribution of a random variable X is defined as:

$$F(x) = P(X < x) \tag{3}$$

The probability density function (p.d.f.) is the derivative of:

$$f(x) = \frac{dF(x)}{dx} \tag{4}$$

The expectation operation, which gives the expected value of a function g(x) , is defined as:

$$E\{g(x)\} = \int_{-\infty}^{\infty} g(x) f(x) dx \tag{5}$$

In most cases, the p.d.f. can be decomposed into its constituent moments or cumulants. If a change in condition causes a change in the p.d.f of the signal then the moments and cumulants may also change. The moments of the signal are defined as:

$$m_n = E\{x^n\} \tag{6}$$

where $E\{.\}$ can be estimated.

The most common simple statistical feature used in signal monitoring is the mean square value (second-order moment) of the signal

$$m_2 = \frac{1}{N} \sum_{i=1}^{N} x(i)^2 \tag{7}$$

A second common statistical feature used is the kurtosis which gives an indication of the proportion of samples which deviate from the mean by a small value compared to those which deviate by a large number. The fourth-order moment can be normalized by the second-order moment squared:

$$\gamma_4 = \frac{m_4}{m_2^2} \tag{8}$$

The zero mean Gaussian distributed variable has a kurtosis of 3.

These statistical tools are useful for detecting an incipient failure, while the bispectrum can be used for uniform state system.

B. Wavelet Theory

The continuous wavelet transform (CWT) is defined as follows:

$$C(a,b) = \int_{-\infty}^{+\infty} f(t) \psi_{a,b}(t) dt \tag{9}$$

where

$$\psi_{a,b}(t) = a^{1/2} \psi\left(\frac{t-b}{a}\right) \tag{10}$$

is a window function called the mother wavelet *a* is a scale and *b* is a translation. The term wavelet means a small wave. The smallness refers to the condition that this (window) function is of finite length (compactly supported). The wave refers to the condition that this function is oscillatory. The term mother implies that the functions with different region of support that are used in the transformation process are derived from one main function, or the mother wavelet. In other words, the mother wavelet is a prototype for generating the other window functions.

Wavelet packets consist of a set of linearly combined usual wavelet functions. The wavelet packets inherit the properties such as orthonormality and time-frequency localization from their corresponding wavelet functions. A wavelet packet $\psi^i_{j,k}(t)$ is a function with three indices where integers i, j and k are the modulation, scale and translation parameters, respectively,

$$\psi^i_{j,k}(t) = 2^{j/2} \psi^j (2^j t - k), \quad \mathrm{i} = 1,2,3,... \tag{11}$$

The wavelet packet component signal $f^i_j(t)$ can be represented by a linear combination of wavelet packet functions $\psi^i_{j,k}(t)$ as follows:

$$f^i_j(t) = \sum_{k=-\infty}^{\infty} c^i_{j,k}(t) \psi^i_{j,k}(t) \tag{12}$$

where the wavelet packet coefficients $c^i_{j,k}(t)$ can be obtained from

$$c_{j,k}^{i}(t)=\int_{-\infty}^{+\infty} f(t)\psi_{j,k}^{i}(t)dt \tag{13}$$

and

$$f(t)=\sum_{i=1}^{2j} f_j^i(t) \tag{14}$$

The wavelet packet energy index is used to identify the initial locations of damage. In this case, the signal energy E_{f_j} at j level is first defined as:

$$E_{f_j}=\int_{-\infty}^{+\infty} f^2(t)dt=\sum_{m=1}^{2^j}\sum_{n=1}^{2^j}\int_{-\infty}^{+\infty} f_j^m(t)f_j^n(t)dt \tag{15}$$

After manipulations is possible to find the wavelet packet component $E_{f_j^i}$ as the stored energy in the component signal $f_j^i(t)$ as:

$$E_{f_j^i}=\int_{-\infty}^{+\infty} f_j^i(t)^2 dt \tag{16}$$

The wavelet packet energy rate index is used to indicate the localization of the structural damage. The rate of signal wavelet packet energy $\Delta(E_{f_j})$ at j level is defined as

$$\Delta(E_{f_j})=\sum_{i=1}^{2^j}\frac{\left|(E_{f_j^i})_b-(E_{f_j^i})_a\right|}{(E_{f_j^i})_a} \tag{17}$$

where $(E_{f_j^i})_a$ is the component signal energy $E_{f_j^i}$ at j level without damage, and $(E_{f_j^i})_b$ is the component signal energy $\mathrm{E}_{\mathrm{f}_\mathrm{j}^\mathrm{i}}$ with some damage.

C.PSO Method

In this work the physical parameters of a steel clamped-free; clamped-clamped and free-free beam are estimated using measured and numeric frequency response functions (FRFs). The mathematical models are obtained using the finite element method (FEM). To approximate the experimental and numeric FRF data the Particle Swarm Optimizer method (PSO) is used. The PSO algorithm is a biologically-inspired algorithm motivated by a social analogy. Sometimes it is related to the Evolutionary Computation (EC) techniques, basically with Genetic Algorithms (GA) and Evolutionary Strategies (ES), but there are significant differences with those techniques. The PSO algorithm is population-based: a set of potential solutions evolves to approach a convenient solution (or set of solutions) for a problem. Being an optimization method, the aim is finding the global optimum of a real-valued function (fitness function) defined in a given space (search space).

In the PSO algorithm each individual is called a "particle", and is subject to a movement in a multidimensional space that represents the belief space. Particles have memory, thus retaining part of their previous state. There is no restriction for particles to share the same point in belief space, but in any case their individuality is preserved. Each particle's movement is the composition of an initial random velocity and two randomly weighted influences: individuality, the tendency to return to the particle's best previous position, and sociality, the tendency to move towards the neighborhood's best previous position.

The "continuous" version uses a real-valued multidimensional space as belief space, and evolves the position of each particle in that space using the following equations:

$$v_i(k+1)=v_i(k)+\gamma_{1i}(p_i-x_i(k))+\gamma_{2i}(G-x_i(k)) \tag{18}$$

$$x_i(k+1)=x_i(k)+v_i(k+1) \tag{19}$$

where: i is the particle index; k is the discrete time index; v is the velocity on i[th] particle; x is the position of the i[th] particle; p is the best position found by i[th] particle (personal best); G is the best position found by swarm (global best, best of personal bests); $\gamma_{1,2}$ are random numbers on the interval [0,1] applied to i[th] particle..

D.Modal Parameters

In the identification of damage (structural changes) are also used methods considering the modal changes. A method of setting modal (Modal Assurance Criterion - MAC) is used to compare pairs of modes. The matrix coefficients are obtained by [21]:

$$MAC_{i,j}=\frac{\left(\{\phi_A\}_i^T\{\phi_A\}_j^*\right)^2}{\{\phi_A\}_i^T\{\phi_A\}_i^*\{\phi_X\}_j^T\{\phi_X\}_j^*} \tag{20}$$

where $\{\phi_A\}$ and $\{\phi_X\}$ denotes the numeric and experimental modes; the superscript symbol T denotes the transpose of a vector and the subscript superscript symbol * denotes the complex conjugate vector.

A MAC value close to 1 suggests that the two modes are well correlated. An overall mode shape indicator may be calculated from:

$$\varepsilon_{\phi} = \left[1 - \frac{1}{L}\sqrt{\sum_{i=1}^{L}(MAC)_i^2} \right] \times 100 \tag{21}$$

III. RESULTS

The geometric dimensions of the experimental clamped-free, clamped-clamped and free-free beam steel sample are: length = 0.84m; thickness = 0.0127m and width = 0.0254m. The effective length for the conditions clamped-free and clamped-clamped is 0.825m.

The experimental data are obtained using the impact hammer and one accelerometer displaced along the sample in the positions 0.125m; 0.225m; 0.325m; 0.425m; 0.525m; 0.625m; 0.725m and 0.825m for the clamped-free beam; 0.125m; 0.225m; 0.325m; 0.425m; 0.525m; 0.625m and 0.725m for the clamped-clamped beam, and 0.105m; 0.21m; 0.315m; 0.42m; 0.525m; 0.63m and 0.735m for the free-free beam.

The first step was to obtain data in the frequency domain and time domain. The data in the frequency domain are used to obtain the modal parameters and data in the time domain are used for application of statistical methods. The inverse of FRF was used with the intention that the signals had the same amplitude of excitation force.

The structural modifications were introduced in positions near 0.0725m (clamped-free and clamped-clamped beam) and 0.0825m (free-free beam). For these three cases the data were collected for the system with and without damage with three levels of damage.

In an attempt to identify the damage, we applied the bispectrum technique in the signal in time domain. Figs. 1 and 2 show the bispectrum of the signal at position 0.425m for the system (clamped-free beam) with and without damage. The curves present differences but is visually difficult to establish a reliable parameter for analysis.

To overcome this problem, it was defined a relative parameter contained the sum of all values of the bispectrum defined by (2):

$$IndB = \sum_{i=1}^{n} b(k,l) \tag{22}$$

$$Brel = \frac{\left|IndB_b - IndB_a\right|}{\left|IndB_a\right|} \tag{23}$$

where $IndB_b$ is the bispectrum parameter of the system with damage and $IndB_a$ is the bispectrum parameter of the system without damage.

Figs. 3 to 5 show the values of the parameter B_{rel} for all position of the accelerometer. Fig. 3 shows the curves for the system clamped-free; Fig. 4 for the system free-free and Fig. 5 for the system free-free. It can be noticed that the great values for all cases of damage are found for the position 1 of the accelerometer. In all situations the great values correspond to the real near position of the damages. Similar results are found for all 3 systems (Figs. 6-8) when using the energy index defined by (17). In these Figs. 3 to 8 the solid line represents damage 1; discontinuous line damage 2 and dotted line damage 3.

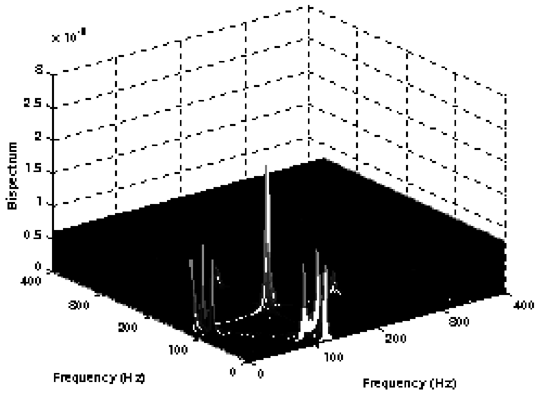

Fig. 1 Bispectrum (system without damage)

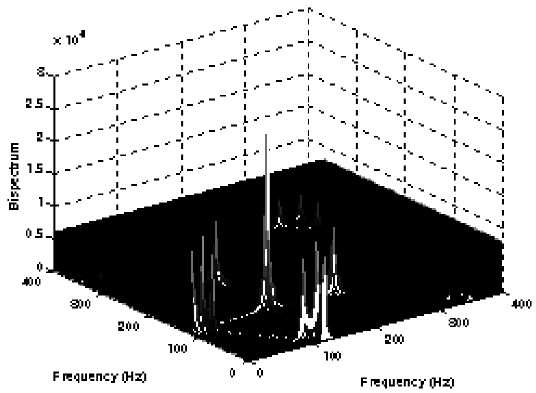

Fig. 2 Bispectrum (system with damage)

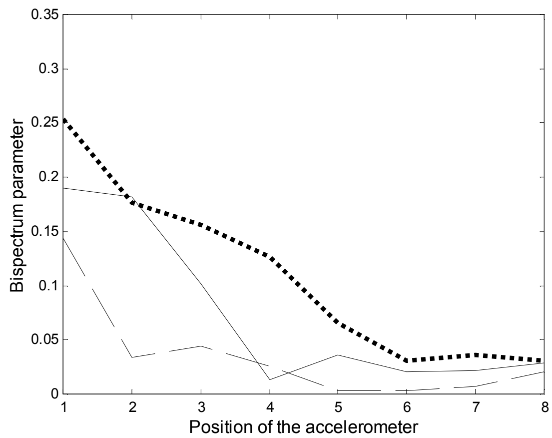

Fig. 3 Bispectrum (clamped-free beam)

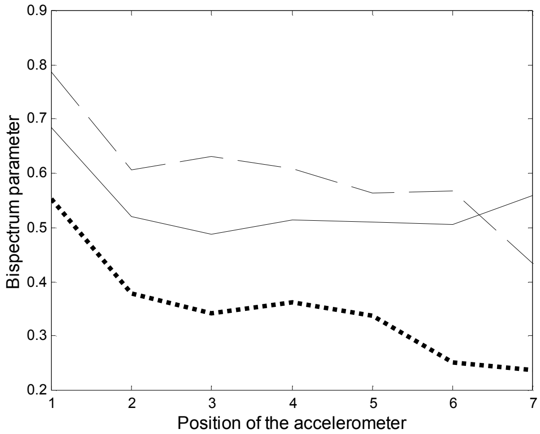

Fig. 4 Bispectrum (clamped-clamped beam)

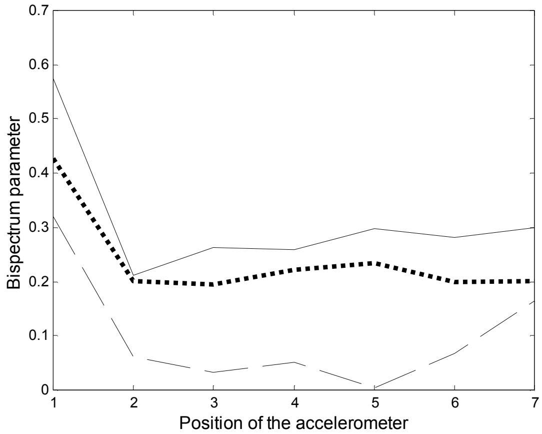

Fig. 5 Bispectrum (free-free beam)

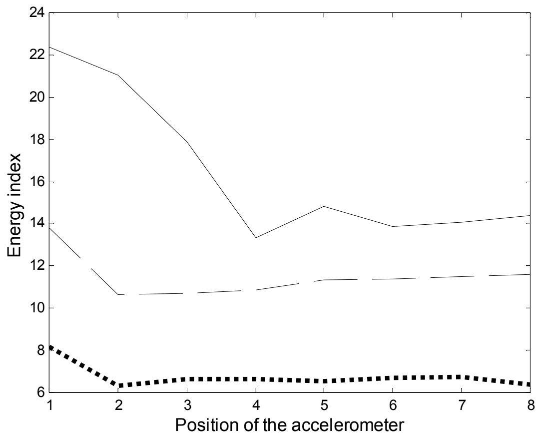

Fig. 6 Energy index (clamped-free beam)

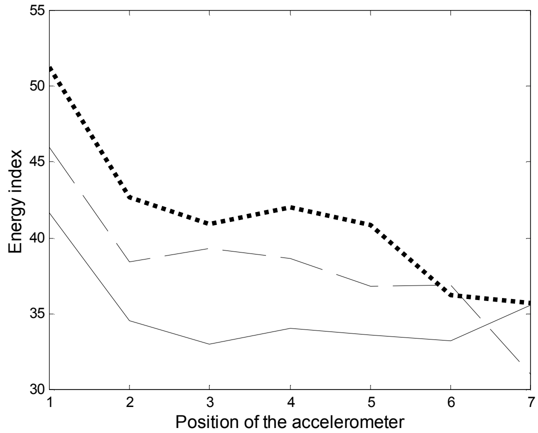

Fig. 7 Energy index (clamped-clamped beam)

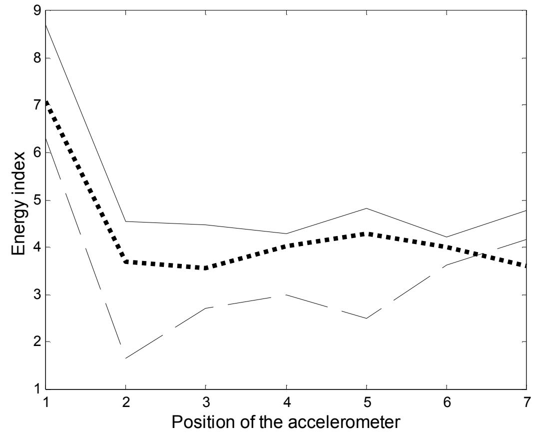

Fig. 8 Energy index (clamped-clamped beam)

After the verification of the approximated position of the damage it was obtained a mathematical model of the beam through the finite element method for the three boundary conditions. The influence of the severity degree of damage was also evaluated. The MAC number (20) e the error parameter (21) it was used to validate the numeric and experimental data. Tables I to III show the values of these parameters for the beam system with three different boundary conditions. The maximum error is of the order of 0.5 % obtained for the free-free system.

TABLE I
MAC NUMBER (CLAMPED-FREE BEAM)

System	1st mode shape	2nd mode shape	3rd mode shape	Error
No damage	0.9997	0.9987	0.9990	0.0855
Damage 1	0.9996	0.9987	0.9994	0.0767
Damage 2	0.9999	0.9993	0.9991	0.0571
Damage 3	0.9998	0.9985	0.9989	0.0938

TABLE II
MAC NUMBER (CLAMPED-CLAMPED BEAM)

System	1st mode shape	2nd mode shape	3rd mode shape	Error
No damage	0.9999	0.9998	0.9971	0.1065
Damage 1	0.9999	0.9995	0.9983	0.0761

Damage 2	0.9998	0.9996	0.9951	0.1800
Damage 3	0.9997	0.9990	0.9961	0.1698

TABLE III
MAC NUMBER (FREE-FREE BEAM)

System	1st mode shape	2nd mode shape	3rd mode shape	Error
No damage	0.9991	0.9989	0.9967	0.1751
Damage 1	0.9989	0.9969	0.9915	0.4237
Damage 2	0.9995	0.9964	0.9890	0.5034
Damage 3	0.9987	0.9989	0.9975	0.1634

Finally, we tried to adjust the possible location of the damage based on the variations of natural frequencies and a performance index defined by (22). To adjust the position of the damage, it was made a sweep of the damage position along the sample. The position analyzed is according to position of the accelerometers showed in Figs. 3 to 8. As the greater levels of energy are near to the first accelerometer, it was considered the damage position varying between 0 to the position in the middle of the first and second accelerometer. Figs. 9 to 11 show the variation of the first, second and third natural frequencies considering the damage with length of 1mm and the height varying of 1 to 5mm.

The numerical and experimental data are approximated using the Particle Swarm Optimizer (PSO) method and this way is possible to adjust the localization and the severity of the damage were considered the first three natural frequencies and the following parameter error checking was used:

$$\varepsilon_{\omega} = \left[\frac{\sum_{i=1}^{L} \left(\omega_{A_i} - \omega_{X_i} \right)^2}{\sum_{i=1}^{L} \omega_{A_i}^2} \right]^{1/2} \tag{24}$$

where ω_{A_i} and ω_{X_i} represent the experimental and numeric frequencies. Three input variables were used in the optimizing process: position, length and height of the damage.

The optimized parameters for the three systems are show in Tables IV, V, and VI. The fitted parameters shown in Tables IV, V, and VI and the real parameters (reference values) present good agreement. The PSO parameters used are: particles number: 25; velocity 2; acceleration constant: 2.1; inertia weights: 0.9 and 0.6 and number of iterations: 400. The convergence demands great computational time because it was used a finite element mesh with elements of 16 nodes and 1mm of size.

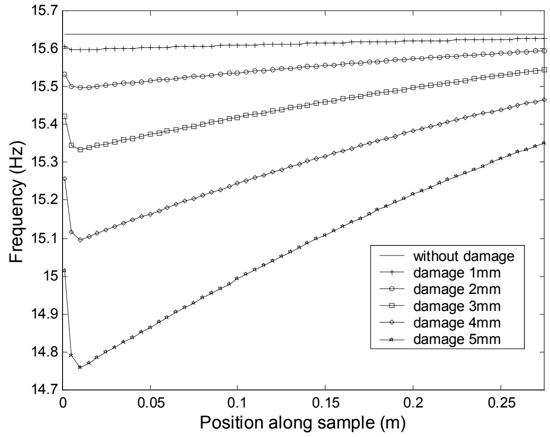

Fig. 9 First natural frequency (clamped-free beam)

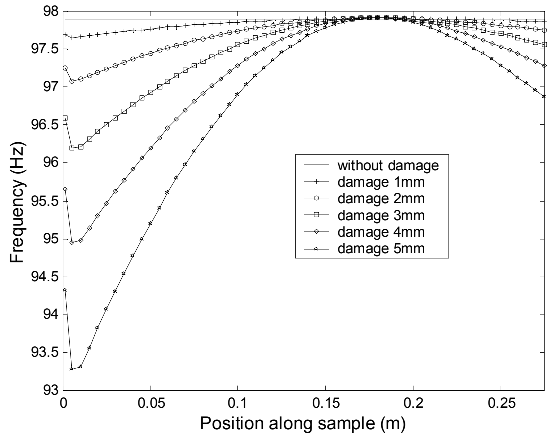

Fig. 10 Second natural frequency (clamped-free beam)

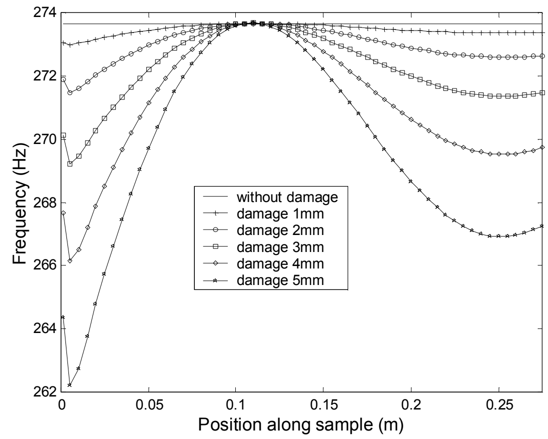

Fig. 11 Third natural frequency (clamped-free beam)

TABLE IV
OPTIMIZED DAMAGE PARAMETERS (CLAMPED-FREE BEAM)

	Position (m)	Length (m)	Height (m)
Damage1	0.0745	0.0010	0.00095
Damage2	0.0751	0.0011	0.00249
Damage3	0.0750	0.0011	0.00457

Reference values	0.0750	0.0010	0.00100 0.00250 0.00450

TABLE V
OPTIMIZED DAMAGE PARAMETERS (CLAMPED-CLAMPED BEAM)

	Position (m)	Length (m)	Height (m)
Damage1	0.0845	0.0011	0.00097
Damage2	0.0852	0.0010	0.00255
Damage3	0.0851	0.0011	0.00452
Reference values	0.0850	0.0010	0.00100 0.00250 0.00450

TABLE VI
OPTIMIZED DAMAGE PARAMETERS (FREE-FREE BEAM)

	Position (m)	Length (m)	Height (m)
Damage1	0.0755	0.0009	0.00095
Damage2	0.0770	0.0011	0.00248
Damage3	0.0765	0.0011	0.00449
Reference values	0.0760	0.0010	0.00100 0.00250 0.00450

IV. CONCLUSION

It was noted that the application of statistical methods for assessing damage to structures can be a potential tool. The specific application for cantilever beams presents difficulties due to variations in the vibration modes of the system. It was observed large variations in values of the bispectrum and the energy index and it was not possible to establish a trend of increasing or decreasing values with the variation in the level of damage and its location. The two parameters presented good estimative of the position of the damage.

The damage position in the sample was obtained considering a procedure of minimization of a performance index based on the correlation of numerical and experimental natural frequencies. To adjust the position of the damage, it was made a sweep of the damage position along the sample using the PSO method. The numeric damage position and the optimal geometric damage parameters are close to the real values.

REFERENCES

[1] E. P. Carden, and P. Fanning, "Vibration Based Condition Monitoring: A Review", *Structural Health Monitoring,* vol. 3, pp. 355-377, 2004.

[2] W. Fan and P. Qiao, "Vibration-based Damage Identification Methods: A Review and Comparative Study", *Structural Health Monitoring,* vol. 10, pp. 83-111, 2010.

[3] A. Alvandi and C. Cremona, "Assessment of vibration-based damage identification techniques", *Journal of Sound and Vibration*, vol. 292, pp. 179-202, 2006.

[4] I. Bovio, *Innovative method for damage identification and structural health monitoring based on vibration measurements*., Doctor Thesis, Università degli Studi di Napoli " Federico II", 238p, 2000.

[5] S. Dincal, *Structural damage detection using frequency response functions*, Master Dissertation, Texas A&M University, 164p, 2005.

[6] A. Rivola and P. R. White, "Bispectral analysis of the bilinear oscillator with application to the detection of fatigue cracks", *Journal of Sound and Vibration*, vol. 216, pp. 889-910, 1998.

[7] H. R. E. Siller, *Non-Linear Modal Analysis Methods for Engineering Structures*, PHd. Thesis, Imperial College London/University of London, 242 p. , 2004.

[8] Y.J.,Yan, L. Chen, Z. Y. Wu and L. H. Yam, "Development in vibration-based structural damage detection technique", *Mechanical Systems and Signal Processing*, vol.. 21, pp. 2198-2211, 2007.

[9] M. Choi and B. Sweetman, "Efficient Calculation of Statistical Moments for Structural Health Monitoring", *Structural Health Monitoring,* vol. 9, pp. 13-24, 2010.

[10] A. L. Cundy, *Use of response surface metamodels in damage identification of dynamic structures*, Master Dissertation, Virginia Polytechnic Institute and State University, 77p, 2003.

[11] S. G. Mattson and S. M. Pandit, "Statistical moments of autoregressive model residuals for damage localization", *Mechanical Systems and Signal Processing*, vol. 20, pp. 627-645, 2006.

[12] McCormick, A. C. (1998). Cyclostationary and higher-order statistical signals processing algorithms for machine condition monitoring. Doctor Thesis. University of Strathclyde. 160 p.

[13] M. L. Fugate, H. Sohn and C. R. Farrar, "Vibration-based damage detection using statistical process control", *Mechanical Systems and Signal Processing*, vol. 15, pp. 707-721, 2001.

[14] Y. Xia and H. Hao, "Statistical damage identification of structures with frequency chances", *Journal of Sound and Vibration*, vol. 263, pp. 853-870, 2003.

[15] H. Khatam, A. A. Golafshani, S. B. Beheshti-Aval, and M. Noori, **"**Harmonic Class Loading for Damage Identification in Beams Using Wavelet Analysis", *Structural Health Monitoring,* vol. 6, pp. 67-80., 2007.

[16] A. Shinde and Z. Hou, "A Wavelet Packet Based Sifting Process and its Application for Structural Health Monitoring", *Structural Health Monitoring,* vol. 4, pp. 153-170, 2005.

[17] M. M. R. Taha, A. Noureldin, J. L. Lucero and T. J. Baca, "Wavelet Transform for Structural Health Monitoring: A Compendium of Uses and Features", *Structural Health Monitoring,* vol. 5, pp. 267-295, 2006.

[18] H. Grafe, *Model updating of large structural dynamics models using measured response functions*, PhD Thesis, Imperial College London/ University of London, 184p. , 1998.

[19] R. Perera and A. Ruiz, "A multistage FE updating procedure for damage identification in large-scale structures based on multiobjective evolutionary optimization", *Mechanical Systems and Signal Processing*, vol. 22, pp. 970-991, 2008.

[20] R. Perera, S. E. Fang and C. Huerta, "Structural crack detection without updated baseline model by single and multiobjective optimization", *Mechanical Systems and Signal Processing*, vol. 23, pp. 752-768, 2009.

[21] S. Z. Rad, *Methods for updating numerical models in structural dynamics*., PhD Thesis, Imperial College of Science, Technology and Medicine. Department of Mechanical Engineering, 284p, 1997.